crystal structure of **3** is basically the same as that of $Cp_2Nb_2(\mu\text{-}Cl)_2(CO)_4$,[10] where the core is butterfly-shaped.

The reduction of $Cp^*TaCl_2(PhCCPh)$ in THF is rather messy, but in toluene two products are formed cleanly in comparable yields. Spectroscopic and analytical data show these are isomeric dimers with the formula $[Cp^*TaCl(PhCCPh)]_2$. X-ray-quality crystals have not been obtained to date. Work is continuing on these compounds, and the results will be reported later.

The differences between the structures of the carbonyl dimers **1** and **3** and the alkyne dimer **2** are striking. The former have a deeply folded Nb_2Cl_2 core that eclipses the two sets of carbonyl groups on each metal, while in **3** the Nb_2Cl_2 core is planar and the coordinated acetylenes are transoid. The cisoid arrangements in the carbonyl complexes place the π-donor chlorides trans to the π-acceptor carbonyls, an understandable arrangement that leads to increased synergic bonding. But the alkyne group is known to be a powerful electron acceptor also, especially in early-transition-metal complexes. So why are the structures so different?

A possible explanation arises from the difference in the symmetry of the lowest energy acceptor orbitals between a *cis*-$(CO)_2$ grouping and the RCCR group. Figure 4 of ref 10a shows the LUMO's of $CpNbCl_2(PH_3)_2$ and $CpNbCl_2(RCCR)$ fragments. In the phosphine complex, the LUMO is a d_{z^2} orbital directed down between the legs of the four-legged piano stool. Adding an electron to the LUMO to make a Nb(II) radical would lead to a Nb–Nb bond along the z axis and give the highly folded structure observed. (The two chloride ligands of each "$CpNbCl_2L_2$" fragment are shared, but this does not disturb the symmetry of the metal fragment.) Conversely, the LUMO of the $CpNbCl_2(RCCR)$ fragment is an $x^2 - y^2$ orbital pointing *between* the chloride ligands. Formation of a Nb–Nb bond with this orbital will give rise to the planar Nb_2Cl_2 core. Thus, if the LUMO of a $CpNbCl_2(CO)_2$ fragment resembles that of $CpNbCl_2(PH_3)_2$, the different Nb(II) structures can be readily rationalized. See ref 10a for a fuller description of the symmetry properties of the ligands that lead to the different LUMO's.

The homometallic dimers **1–3** provide examples of niobium and tantalum complexes in the relatively rare +2 oxidation state, and they are promising starting points for the study of the chemistry of Nb(II) and Ta(II) complexes with carbonyl and alkyne ligands.

Acknowledgment. We thank the donors of the Petroleum Research Fund, administered by the American Chemical Society, and the National Science Foundation (Grant CHE-8619864) for support of this research.

Supplementary Material Available: Tables VIIIS–XS (thermal parameters for **1**, **2a**, and **3**) and Tables XIS–XIIIS (bond angles for **1**, **2a**, and **3**) (5 pages); Tables XIVS–XVIS (F_o vs F_c for **1**, **2a**, and **3**) (45 pages). Ordering information is given on any current masthead page.

Photoelectron Spectroscopy and Rates of CO Substitution of $(\eta^5\text{-}C_5H_4X)Rh(CO)_2$ Compounds. Separation of σ and π Ring Substituent Effects

Dennis L. Lichtenberger* and Sharon K. Renshaw

Laboratory for Electron Spectroscopy and Surface Analysis, Department of Chemistry, The University of Arizona, Tucson, Arizona 85721

Fred Basolo* and Minsek Cheong

Department of Chemistry, Northwestern University, Evanston, Illinois 60208

Received April 9, 1990

The He I photoelectron spectra for a series of monosubstituted $(\eta^5\text{-}C_5H_4X)Rh(CO)_2$ compounds are reported (where X = NO_2, CF_3, Cl, H, CH_3, NMe_2) and compared to the rates of carbonyl substitution reactions. The carbonyl substitution by phosphine follows an associative mechanism, and the rates are generally inhibited by greater electron richness at the metal center in these compounds. However, the rates for certain substitutions, particularly when X is Cl or NMe_2, are faster than indicated by the inductive characteristics of these groups. The photoelectron spectra of the $(\eta^5\text{-}C_5H_4X)Rh(CO)_2$ compounds illustrate the effects of X on the electronic structure and rates of substitution. Pronounced shifts are seen in the cyclopentadienyl π and metal d valence ionizations as the X group is varied. The shifts of most of the valence ionizations closely follow the inductive capabilities of the X substituents, as also indicated by correlations with Hammett σ values and the carbonyl stretching frequencies of the compounds. Certain ionizations are also affected by orbitals of the X group that have π symmetry with respect to the cyclopentadienyl ring. Thus, the ionization energy shifts provide a relative measure of the inductive and resonance (π) interaction between X and the compound. The rates of CO substitution correlate with the ionizations when the shifts due to both the inductive and resonance (π) effects are taken into account. These results suggest that the "slipped ring" intermediate $(\eta^3\text{-}C_5H_4X)Rh(CO)_2PPh_3$ is stabilized through π delocalization on the cyclopentadienyl ring, thus enhancing the rates of substitution.

Introduction

Associative substitution in 18-electron organometallic compounds can be facilitated if a pair of electrons is easily localized on a ligand, thereby releasing a coordination site at the metal.[1] If the molecule contains a cyclopentadienyl ring (Cp), one mechanism for freeing a coordination site is for the Cp ring to "slip" from η^5 to η^3 coordination, leaving the other two Cp π electrons localized in a carbon–carbon bond:[2]

* To whom correspondence should be addressed.

(1) (a) Basolo, F. *Inorg. Chim. Acta* **1985**, *100*, 33. (b) Basolo, F. *Inorg. Chim. Acta* **1981**, *50*, 65.

0276-7333/91/2310-0148$02.50/0

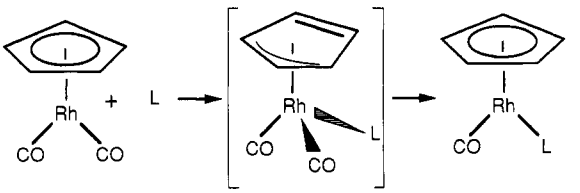

Such a mechanism has been proposed in the associative substitution of CO in the compounds $(\eta^5\text{-}C_5H_5)M(CO)_2$ (M = Co, Rh).[2] The role of η^3-Cp coordination in associative substitution has since been investigated by perturbing the electronic structure of the Cp ring.[3,4] The most systematic study examined a series of compounds that contain a range of electron-withdrawing or -releasing functional groups on the cyclopentadienyl ring.[5] The compounds $(\eta^5\text{-}C_5H_4X)Rh(CO)_2$, where X = NO_2, CF_3, Cl, H, CH_3, NMe_2, all react with PPh_3 to replace a carbonyl via an associative mechanism:[6]

$$(\eta^5\text{-}C_5H_4X)Rh(CO)_2 + PPh_3 \rightarrow (\eta^5\text{-}C_5H_4X)Rh(CO)(PPh_3) + CO \quad (1)$$

$$X = NO_2,\ CF_3,\ Cl,\ H,\ CH_3,\ NMe_2$$

The observed rates of CO substitution have been compared with several other properties of the compounds.[5] The carbonyl stretching frequencies (ν_{CO}) of the compounds correlate linearly with the Hammett σ_p parameters of the X groups, indicating that each gives a consistent measure of the relative electron richness at the metal center. The rates are expected to decrease when there is greater negative charge at the metal center; however, the rates of CO substitution do not correlate in every case to the Hammett σ_p parameters or carbonyl stretching frequencies. The trend is true only for compounds with X = NO_2, CF_3, H, CH_3. The rates for the Cl and NMe_2 compounds are considerably faster than expected on the basis of the Hammett σ_p parameter of these groups. The effects of solvents, steric factors, or other macroscopic contributions were considered to be relatively less important in comparing the rates of this series of compounds. The disproportionate rate increase for the Cl and NMe_2 compounds was proposed to be a consequence of an orbital overlap between the p_π lone pair on the X group and the π system of the Cp ring, which would stabilize the η^3-Cp intermediate:

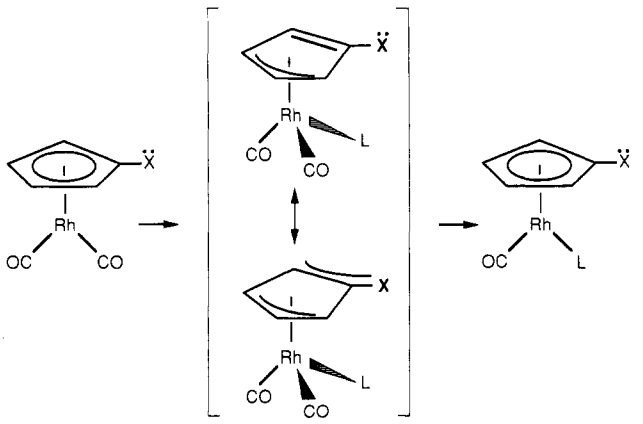

Photoelectron spectroscopy (PES) provides a direct experimental measure of separate σ (inductive) and π (resonance) bonding capabilities.[7,8] In this case, PES of the $(\eta^5\text{-}C_5H_4X)Rh(CO)_2$ compounds can measure the σ and π interactions of the X group with the Cp ring. The photoelectron spectra also show the influences of the X group on the bonding and electron distribution in the rest of the compound. The relative shifts of the ionization bands allow us to investigate separate inductive (σ) and resonance (π) effects on the experimental rates of CO substitution. The resulting correlation supports the contribution of a stabilized η^3-coordinated Cp in the transition state of the associative substitution.

Experimental Section

The syntheses and characterization of the rhodium compounds $(\eta^5\text{-}C_5H_4X)Rh(CO)_2$ have been published previously.[5] Photoelectron spectra were recorded with an instrument that features a 36-cm hemispherical analyzer (10-cm gap) and custom-designed sample cells, excitation sources, and detection and control electronics. The instrumentation and data collection methods have been described previously.[9] The photoelectron spectra of liquid samples (X = CF_3, Cl, CH_3) were obtained at room temperature (27 °C) with an external gas inlet system. The spectra of monosubstituted benzenes C_6H_5X (X = Cl, NMe_2, NO_2) were also collected under these conditions for comparison with those of the rhodium compounds. The spectra of solid samples (X = NO_2, NMe_2) were obtained at 30 °C with an internal sample cell. All samples vaporized cleanly, with no detectable evidence of decomposition products in the gas phase or as a solid residue. Resolution was <0.025 eV (fwhm of Ar $^2P_{3/2}$) during collection. The He II spectra were obtained with a custom-designed charged-particle oscillator source and referenced to the He^+ ionization (with resolution fwhm of He^+ <0.050 eV during collection). All data were intensity-corrected with an experimentally determined instrument analyzer sensitivity function. The He II data were also corrected for the He II β excitation line.

The valence ionization bands are represented analytically with the best fit (program GFIT)[10] of asymmetric Gaussian peaks.[10,11] The bands are defined with the position, amplitude, half-width for the high binding energy side of the peak, and half-width for the low binding energy side of the peak (see Table I). The peak positions were determined in a precise and consistent manner for correlation with the reactivity of the compounds. The peak positions and half-widths are reproducible to about ±0.02 eV ($\sim 3\sigma$ level). The confidence limits for the relative integrated peak areas are about 10%, with the primary source of uncertainty being the determination of the base line subtracted from the peak. The parameters describing an individual ionization peak are less certain when two or more peaks are close in energy and are overlapping. If the combined band contour does not contain sufficient information for independent determination of the individual peak parameters, the number of peaks and/or independent parameters in the analytical representation is appropriately reduced.[10,11] These situations are discussed in the Results and are evident in the tables, where half-widths for similar peaks are occasionally constrained to be the same. In every case but one where a Gaussian component is displayed, there is an observable peak or shoulder in the spectrum corresponding to that component. The one exception is the M3 and R1 ionizations of the complex with X = Cl, which are too close in energy to give separable features.

(2) Schuster-Woldan, H. G.; Basolo, F. *J. Am. Chem. Soc.* **1966**, *88*, 1657.
(3) Rerek, M. E.; Basolo, F. *Organometallics* **1983**, *2*, 372.
(4) Rerek, M. E.; Basolo, F. *J. Am. Chem. Soc.* **1984**, *106*, 5908.
(5) Cheong, M.; Basolo, F. *Organometallics* **1988**, *7*, 2041.
(6) The substitutions were all first order in PPh_3 and first order in complex and had activation parameters of $\Delta H^* < 20$ kcal/mol and $\Delta S^* < -15$ eu. Complete kinetic data are reported in ref 5.

(7) Lichtenberger, D. L.; Kellogg, G. E. *Acc. Chem. Res.* **1987**, *20*, 379.
(8) Lichtenberger, D. L.; Kellogg, G. E.; Pang, L. S. K. *Experimental Organometallic Chemistry*; ACS Symposium Series 357; American Chemical Society: Washington, DC, 1987; p 265.
(9) (a) Calabro, D. D.; Hubbard, J. L.; Blevins, C. H., II; Campbell, A. C.; Lichtenberger, D. L. *J. Am. Chem. Soc.* **1981**, *103*, 6739. (b) Lichtenberger, D. L.; Kellogg, G.; Kristofszki, J. G.; Page, D.; Turner, S.; Klinger, G.; Lorenzen, J. *Rev. Sci. Instrum.* **1986**, *57*, 2366. (c) Hubbard, J. L. *Diss. Abstr. Int.* **1983**, *43*, 2203.
(10) Lichtenberger, D. L.; Fenske, R. F. *J. Am. Chem. Soc.* **1976**, *98*, 50.
(11) (a) Lichtenberger, D. L.; Copenhaver, A. S. *J. Electron Spectrosc. Relat. Phenom.* **1990**, *50*, 335. (b) Copenhaver, A. S. Dissertation, University of Arizona, 1989.

Table I. Results of Fits of PES Data for $(\eta^5\text{-}C_5H_4X)Rh(CO)_2$ Compounds

X	IP, eV	half-width, eV		rel peak area			label
		high energy	low energy	He I	He II	He I/He II	
NO_2	8.19	0.65	0.26	1.00			M1
	9.15	0.51	0.21	0.86			M2
	10.00	0.49	0.39	1.05			M3
	10.34	0.49	0.39	1.66			R1
	10.77	0.58	0.42	2.42			$M4/NO_2$ LP
	11.21	0.58	0.42	1.92			R2
Cl	7.73	0.58	0.26	1.00	1.00	1.00	M1
	8.75	0.44	0.19	0.82	1.38	1.68	M2
	9.48	0.46	0.41	1.31	1.13	0.86	R1
	9.81	0.46	0.41	0.98	1.03	1.05	M3
	10.30	0.63	0.38	1.08	1.27	1.18	M4
	10.63	0.63	0.38	1.03	0.79	0.77	R2
CF_3	7.97	0.61	0.27	1.00			M1
	8.94	0.53	0.20	0.89			M2
	9.78	0.36	0.34	0.74			M3
	10.12	0.55	0.36	1.37			R1
	10.59	0.72	0.36	1.03			M4
	10.92	0.71	0.32	0.86			R2
NMe_2	7.18	0.50	0.46	1.00			M1
	7.99	0.55	0.39	0.72			M2
	8.34	0.58	0.39	1.48			R1
	9.12	0.53	0.46	0.88			M3
	9.72	0.53	0.46	0.91			M4
	10.08	0.65	0.40	1.12			R2
	10.51	0.56	0.33	1.26			NMe_2 LP
H	7.63	0.50	0.22	1.00	1.00	1.00	M1
	8.65	0.42	0.16	0.87	1.40	1.61	M2
	9.50	0.43	0.33	1.03	1.62	1.57	M3
	9.82	0.43	0.33	1.21	0.70	0.58	R1
	10.25	0.54	0.34	1.05	0.83	0.79	M4
	10.59	0.54	0.34	1.01	0.71	0.70	R2
CH_3	7.45	0.57	0.25	1.00	1.00	1.00	M1
	8.52	0.45	0.18	0.85	1.32	1.56	M2
	9.29	0.37	0.34	0.98	1.00	1.02	M3
	9.58	0.48	0.34	1.30	1.01	0.78	R1
	10.07	0.60	0.40	1.21	1.21	1.00	M4
	10.39	0.60	0.40	1.10	0.91	0.83	R2

However, in this case the combined band is too broad for a single ionization, and the slight change in the shape of the band in the He I/He II comparison confirms that more than one ionization is present.

For an analytical representation of the He II data, the position and width values of the asymmetric Gaussians were all constrained to He I values, which are more accurately determined from the He I spectra. The amplitudes were then allowed to vary due to the different cross sections for the He II ionizations.

Results

Photoelectron Spectra and Assignments. The valence photoelectron spectra (6–12 eV) for the series of compounds are shown in Figure 1. The spectra are ordered from the compound with the fastest rate of CO substitution ($X = NO_2$) to the compound with the slowest rate of CO substitution ($X = CH_3$). The valence region is rich in ionizations. It includes, for all six compounds, four bands corresponding to the eight Rh(I) electrons and two bands arising from the orbitals of the e_1'' π combination on the cyclopentadienyl ring. The NO_2 and NMe_2 spectra each have additional ionizations corresponding to orbitals localized on these groups. For purposes of discussion, it is convenient to label the ionizations in terms of their primary parentage in an isolated fragment analysis of the molecular orbitals. The ionizations that trace most directly to rhodium d orbitals are labeled M1 through M4, and those that trace most directly to the e_1'' π levels of an isolated cyclopentadienyl anion are labeled R1 or R2. The ionizations corresponding to the lone pairs of the X groups are labeled LP.

$(\eta^5\text{-}C_5H_5)Rh(CO)_2$. A previous photoelectron study of $(\eta^5\text{-}C_5R_5)M(CO)_2$ compounds (where M = Co, Rh, R = H, CH_3) established the basic electronic structure and assignments for valence ionizations of "two-legged pianostool" compounds.[12] The close-up valence ionization spectrum of $(\eta^5\text{-}C_5H_5)Rh(CO)_2$ is shown in Figure 1. The ionization energies are represented in Figure 2, in relation to the interaction between $[Rh(CO)_2]^+$ and $(C_5H_5)^-$ fragments. The Cp e_1'' orbitals are no longer degenerate in the compound and are labeled e_1^+ and e_1^- according to whether the orbital is symmetric or antisymmetric with respect to the $Rh(CO)_2$ plane. With use of a coordinate system with the $Rh(CO)_2$ fragment in the *yz* plane, the Cp e_1^- orbital overlaps with the d_{xz} orbital and a filled-filled interaction occurs, which results in an antibonding/bonding pair of orbitals. The antibonding combination corresponds to the initial ionization, labeled M1. The He I/He II comparison and shifts with metal and ligand substitution show that the M1 ionization has considerable ligand character.[11] Likewise, the bonding combination corresponds to the sixth ionization (labeled R2) and has a considerable amount of metal character. The ionizations labeled M2, M3, and M4 represent predominantly metal orbitals that back-bond to the carbonyls but have little direct interaction with the Cp ring. Evidence for backbonding of M1 and M2 to the carbonyls is observed in CO vibrational progressions on these ionization bands. Finally,

(12) Lichtenberger, D. L.; Calabro, D. C.; Kellogg, G. E. *Organometallics* 1984, *3*, 1623.

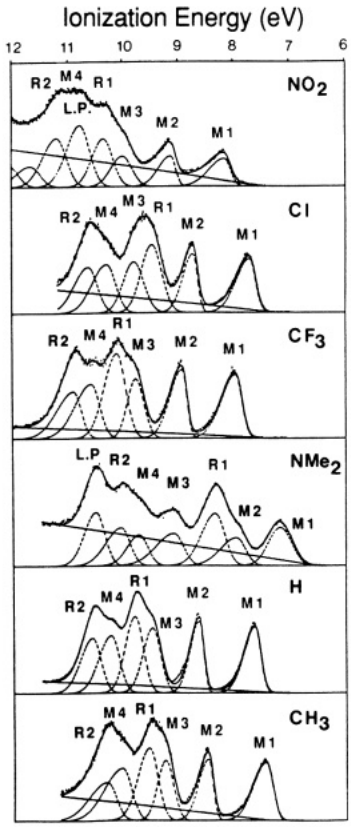

Figure 1. Close-up photoelectron spectra for (η^5-C_5H_4X)$Rh(CO)_2$ (X = NO_2, Cl, CF_3, NMe_2, H, CH_3) ordered from fastest to slowest rate of CO substitution.

the ionization labeled R1 represents the Cp ring e_1^+ orbital, which interacts with the empty metal d_{yz}. This ionization has the largest intensity in the He I spectrum. This is because the He I cross sections for valence ionizations of first-row atoms such as carbon are generally greater than the cross section for the 4d ionizations of rhodium. The labels and predominant orbital characters of these ionizations are summarized in Table II.

Table II. Ionizations of (η^5-C_5H_5)$Rh(CO)_2$

IP, eV	label	primary contribn
7.64	M1	d_{xz}/e_1^-/CO π^* (antibonding combination)
8.65	M2	$d_{x^2-y^2}$/CO π^*
9.50	M3	d_{xy}
9.82	R1	e_1^+
10.25	M4	d_{z^2}
10.59	R2	e_1^-/d_{xz} (bonding combination)

Table III. Ionizations of (η^5-$C_5H_4NMe_2$)$Rh(CO)_2$

IP, eV	label	primary contribn
7.18	M1	d_{xz}/e_1^-
7.99	M2	$d_{x^2-y^2}$/CO π^*/N lone pair
8.34	R1	e_1^+/N lone pair/$d_{x^2-y^2}$
9.12	M3	d_{xy}
9.72	M4	d_{z^2}
10.07	R2	e_1/d_{xz}
10.50	LP	N lone pair

(η^5-$C_5H_4CF_3$)$Rh(CO)_2$. The photoelectron spectrum of (η^5-$C_5H_4CF_3$)$Rh(CO)_2$ is different from the spectrum of (η^5-C_5H_5)$Rh(CO)_2$ only in that the entire valence region has been substantially shifted (by 0.3 eV) to higher binding energy. This stabilization of the ionizations reflects the inductive effect of the electron-withdrawing CF_3 group when it replaces a hydrogen atom on the Cp ring. Other than this stabilization, the spectrum of the CF_3 compound is very similar in appearance to the spectrum of the H compound. There are no significant differences in the separations between ionization bands or in the relative intensities of the bands. Visual examination of the M1 and M2 ionization band shapes shows a high degree of asymmetry with subtle shoulders on the high binding energy sides. Statistical analysis of detailed band shapes as described in ref 11 shows that the M2 band is represented better (with 99% probability by the F test) by three symmetric bands, rather than one asymmetric band. Figure 3 shows the M1 ionization band for the CF_3 compound with the three CO vibrational progressions resulting from back-bonding to the carbonyls. This type of CO vibra-

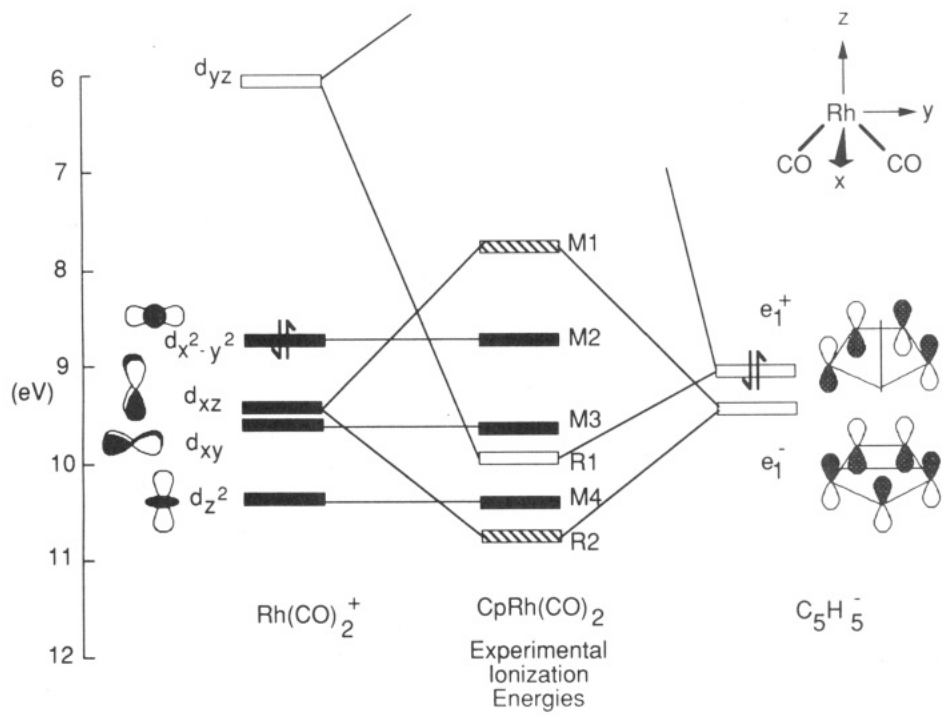

Figure 2. Interaction diagram for $(C_5H_5)^-$ with $Rh(CO)_2^+$. The energy positions for the (η^5-C_5H_5)$Rh(CO)_2$ orbitals (but not the fragment orbitals) are placed at the experimental ionization energies.

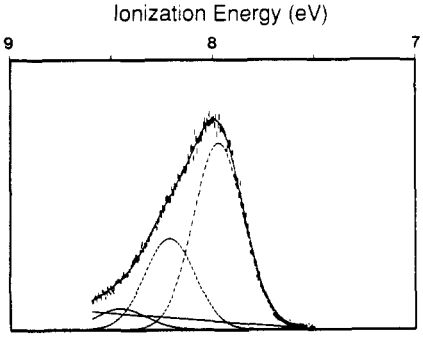

Figure 3. Close-up photoelectron spectrum of the M1 ionization band in $(\eta^5\text{-}C_5H_4CF_3)Rh(CO)_2$, showing vibrational progressions.

tional progression has been seen in the metal-based ionizations of a number of transition-metal carbonyls.[11-13] The assignments for the ionizations are the same as for the $(\eta^5\text{-}C_5H_5)Rh(CO)_2$ compound.

$(\eta^5\text{-}C_5H_4CH_3)Rh(CO)_2$. The spectrum of $(\eta^5\text{-}C_5H_4CH_3)Rh(CO)_2$ shows the entire valence region shifted to lower binding energy from the effects of the electron-donating CH_3 group on the ring. We have discussed in detail this and other electronic effects of methyl substitutions on metal-coordinated Cp rings in previous papers.[14] The $(\eta^5\text{-}C_5H_4CH_3)Rh(CO)_2$ spectrum is similar to the $(\eta^5\text{-}C_5H_5)Rh(CO)_2$ spectrum, with an identical separation between the M1 and M2 ionization bands and similar vibrational progressions on M1 and M2. However, the general features of the remaining group of ionizations change slightly. The assignments in this region are aided by the He I/He II comparisons of relative intensities of the ionization bands, shown in Table I. The He II photoionization cross section for rhodium is quite high compared to that of carbon,[15] causing metal-based peaks to grow in relative intensity in the He II mode relative to the He I mode.[11] In the He II spectrum of the CH_3 compound, the second ionization band shows a large increase in intensity (relative to the first band) and therefore is largely metal in character. The relative He I intensities of the third and fifth ionization bands imply that these are metal-based orbitals with a small amount of interaction with the Cp ring. The fourth and sixth bands decrease in relative intensity and are therefore assigned to Cp-ring-based ionizations. Therefore, the ionization band assignments for the $(\eta^5\text{-}C_5H_4CH_3)Rh(CO)_2$ spectrum are analogous to assignments for the $(\eta^5\text{-}C_5H_5)Rh(CO)_2$ spectrum.

$(\eta^5\text{-}C_5H_4NO_2)Rh(CO)_2$. The valence photoelectron spectrum (Figure 1) of the $(\eta^5\text{-}C_5H_4NO_2)Rh(CO)_2$ compound is more difficult to evaluate due to the presence of ionizations associated with the NO_2 group. The positions and intensities of the first four ionizations are the most certain and they are assigned to M1, M2, M3, and R1, respectively. As will be shown, these are also the most significant ionizations for evaluation of the reactivity. The M1 and M2 ionization bands again have similar splittings as for the other spectra and show evidence of the CO vibrational progressions. The R1 ionization is again relatively intense compared to the metal-based ionizations.

The assignments for the remaining peaks in the spectrum of $(\eta^5\text{-}C_5H_4NO_2)Rh(CO)_2$ are aided by the trends in the series of $(\eta^5\text{-}C_5H_4X)Rh(CO)_2$ compounds and by comparison with the photoelectron spectrum of nitrobenzene. The inductive trends for the series (presented in more detail in the Discussion) support the assignment of R1 to the band at 10.34 eV and the assignment of R2 to the band at 11.21 eV. The assignment of M4 to the band at 10.77 eV also follows the inductive trends of the series. The increased intensity of the region at 10.77 eV indicates that it contains two or more overlapping ionizations and likely includes the ionizations from the NO_2 group. In the photoelectron spectrum of nitrobenzene, the NO_2 group ionizations are located at 11.3 eV ($a_2\pi$) and 11.1 eV ($a_1\sigma$)[16] and have therefore been destabilized by about 0.5 eV in the $(\eta^5\text{-}C_5H_4NO_2)Rh(CO)_2$ compound. This is the expected effect of having the NO_2 bound to a formally negatively charged Cp ring rather than a benzene ring.

$(\eta^5\text{-}C_5H_4NMe_2)Rh(CO)_2$. The spectrum of $(\eta^5\text{-}C_5H_4NMe_2)Rh(CO)_2$ shows the general destabilization of the ionizations to lower binding energy, reflecting inductive effects of the NMe_2 group. This spectrum, however, stands out from the others because of a different pattern of the ionization bands and because of a seventh band corresponding to the nitrogen p_π lone pair. Table III shows the assignments for $(\eta^5\text{-}C_5H_4NMe_2)Rh(CO)_2$. The first two ionizations are comparable to those in $(\eta^5\text{-}C_5H_5)Rh(CO)_2$ and have been similarly assigned to M1 and M2. The band shapes of both ionizations show vibrational progressions. However, the M2 ionization is closer in energy to the M1 ionization than in the spectra of the other compounds. The M4 and R2 bands are assigned analogously to those in $(\eta^5\text{-}C_5H_5)Rh(CO)_2$, on the basis of inductive trends in the series. The third band (at 8.35 eV) is assigned to the R1 (Cp ring e_1^+) ionization partially on the basis of intensity. In the spectra of the other $(\eta^5\text{-}C_5H_4X)Rh(CO)_2$ compounds, the R1 ionization is always the most intense single ionization. Except for the ionization at 10.51 eV (which is in the region expected for the nitrogen p_π lone pair), the third ionization of the NMe_2 compound has the greatest intensity. The R1 ionization has therefore been destabilized by 1.5 eV when the NMe_2 group replaces H on the Cp ring. This destabilization is due in part to the electron-donating effect of the NMe_2 group but is largely due to a p_π overlap (resonance) with the Cp ring. The assignment of the nitrogen lone pair to the ionization at 10.51 eV represents a stabilization relative to *N,N*-dimethylaniline. More will be said in the Discussion.

$(\eta^5\text{-}C_5H_4Cl)Rh(CO)_2$. The photoelectron spectrum of $(\eta^5\text{-}C_5H_4Cl)Rh(CO)_2$, shown in Figure 1, is somewhat similar to the spectrum of $(\eta^5\text{-}C_5H_5)Rh(CO)_2$. The M1 and M2 ionizations are comparable to those in the spectra of the other compounds, with CO vibrational progressions present. The remaining region, however, changes subtly from the analogous regions in the X = CF_3, H, CH_3 spectra. The overlapping R1 and M3 ionizations require special analysis. The combined contour between 9 and 10 eV is too broad for a single ionization and is modeled with two ionizations having half-widths similar to those of the other ionizations of these complexes. As in the other spectra, the ionization with the larger intensity is assigned to R1 (Cp ring e_1^+). In this case, R1 is the third ionization of the complex, similar to the case when X = NMe_2, rather than the fourth ionization as for the other complexes. The placement of R1 and M3 ionizations is further supported by the He II data (Table I), in which the third ionization band (R1) decreases in relative intensity due to the carbon character of the Cp ionization. Conversely, the fourth ionization band (M3) shows little change in intensity, relative to M1, and therefore is metal-based. The R1

(13) (a) Hubbard, J. L.; Lichtenberger, D. L. *J. Am. Chem. Soc.* **1982**, *104*, 2132. (b) Lichtenberger, D. L.; Blevins, C. H. *J. Am. Chem. Soc.* **1984**, *106*, 1636.

(14) Calabro, D. C.; Hubbard, J. L.; Blevins, C. H., II; Campbell, A. C.; Lichtenberger, D. L. *J. Am. Chem. Soc.* **1981** *103*, 6839.

(15) Yeh, J. J.; Lindau, I. *At. Nucl. Data Tables* **1985**, *32*, 7.

(16) (a) Rabalais, J. W. *J. Chem. Phys.* **1972**, *57*, 960. (b) Khalil, O. S.; Meeks, J. L.; McGlynn, S. P. *J. Am. Chem. Soc.* **1973**, *95*, 5876.

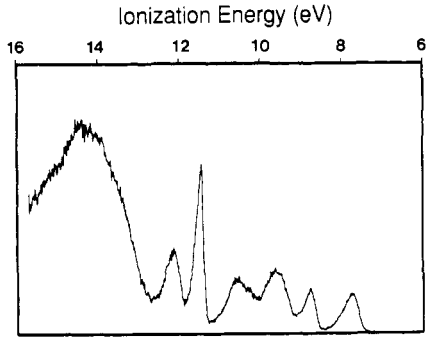

Figure 4. Full valence photoelectron spectrum of $(\eta^5\text{-}C_5H_4Cl)Rh(CO)_2$, showing the ionizations of the chlorine lone pairs.

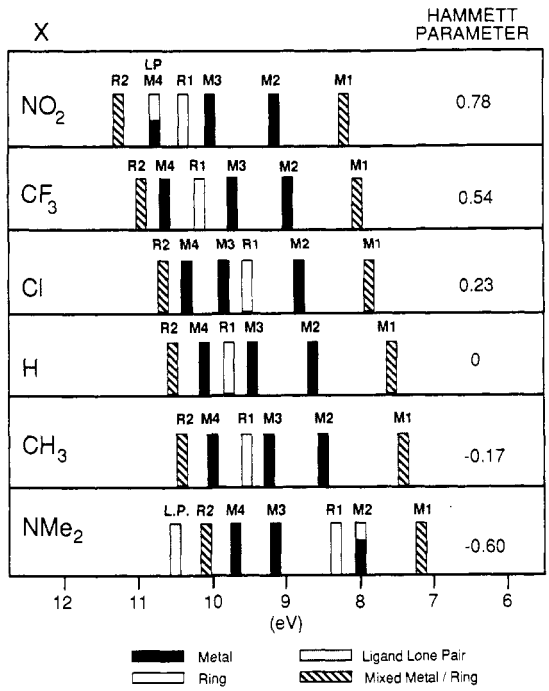

Figure 5. Trends in ionization enegy of the $(\eta^5\text{-}C_5H_4X)Rh(CO)_2$ compounds with use of the assignments shown in Table I. Cross-hatched levels represent orbitals of mixed ring and metal character.

ionization is destabilized by 0.34 eV when Cl replaces H on the Cp ring, due to a combination of inductive and resonance effects. The M4 and R2 ionizations are assigned to be the fifth and sixth bands, which is the same as in the other spectra.

The chlorine lone-pair ionizations also gave important clues about the interaction of Cl with the Cp ring. In the full spectrum of $(\eta^5\text{-}C_5H_4Cl)Rh(CO)_2$, shown in Figure 4, it is easy to locate the two ionizations that arise from the chlorine lone pairs. One is a sharp and very intense band located at 11.44 eV, which is assigned to the p_x orbital. The p_x orbital lies in the plane of the Cp ring and is nonbonding with respect to the π system of the ring. The second band is a broad and less intense band and is located at 12.09 eV. This is assigned to the p_π orbital, which is parallel with the Cp ring π system. The broadness of this band suggests that it has considerable orbital overlap with the Cp. The significance of these positions will also be discussed below.

Discussion

Ionization Energies and the Inductive Effects of the X Substituents. Figure 5 summarizes the assignments of the valence ionizations of the $(\eta^5\text{-}C_5H_4X)Rh(CO)_2$ compounds. The figure lists the compounds in order of decreasing Hammett σ_p values. Note that this is not the same order as the reactivity of the compounds. The inductive effect of the X group is seen in the gradual destabilization of most ionization bands as X becomes a better donor. This inductive effect is most notable for the R2, M2, and M1 ionizations but is also clearly experienced by all valence ionizations of the complexes. The difference between the ionization potentials of R2 and M1 for all the compounds is relatively constant at 2.94 ± 0.06 eV. These two ionizations represent the mixing between the filled ring e_1^- and the filled metal d_{xz}, and the constant separation of these ionizations indicates that varying the X groups does not perturb this interaction significantly. Also note that the separation between the M1 and M2 ionization bands is 1.00 ± 0.04 eV for all compounds except for the NMe_2 compound, which has a separation of 0.78 eV. This destabilization of M2 in the NMe_2 spectrum suggests that this level has an electronic interaction that is not accounted for by the inductive characteristics of the NMe_2 group. More will be said about this later.

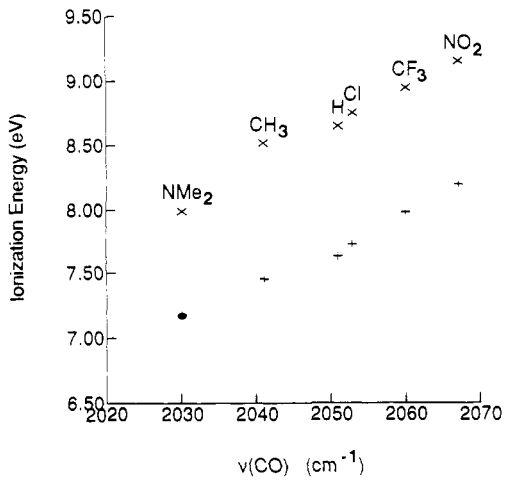

Figure 6. Plot of the M1 (+) and M2 (×) ionization energies versus the symmetric carbonyl stretching frequencies for the series of $(\eta^5\text{-}C_5H_4X)Rh(CO)_2$ compounds.

The inductive effect of the X group is also seen in plots of the M1 and M2 ionization energies versus the carbonyl stretching frequencies (ν_{CO}). Figure 6 shows a plot of the M1 and M2 ionization energies versus the symmetric ν_{CO}'s. The result is two lines with correlation coefficients (R) of 0.9908 (M1) and 0.9852 (M2). Analogous plots were obtained for the antisymmetric ν_{CO}'s with R's of 0.9978 (M1) and 0.9823 (M2). Both the M1 and M2 ionizations show substantial back-bonding to the carbonyls, as seen in the vibrational fine structure on the bands. As charge is donated from the ring to the metal, the M1 orbital is destabilized, which results in increased back-bonding to the carbonyl (lower ν_{CO}). The poorer correlation for the M2 compared to M1 energies is due largely to the relative destabilization of M2 for X = NMe_2.

A plot of M1 and M2 ionization bands versus the Hammett σ_p parameters, shown in Figure 7, also shows a linear relationship. This is an interesting correlation between ionization potentials and parameters based on linear free energy relationships. By definition, the Hammett parameter is reflecting a change in free energy ($\Delta\Delta G$) for benzoic acid dissociation in $C_6H_4(COOH)X$ as the ring substituent is varied.[17] The parameters often correlate to reactions in which the rate varies as a substituent is changed. A linear correlation means that the change in free energy of

(17) March, J. *Advanced Organic Chemistry*, 3rd ed.; Wiley: New York, 1985; Chapter 9.

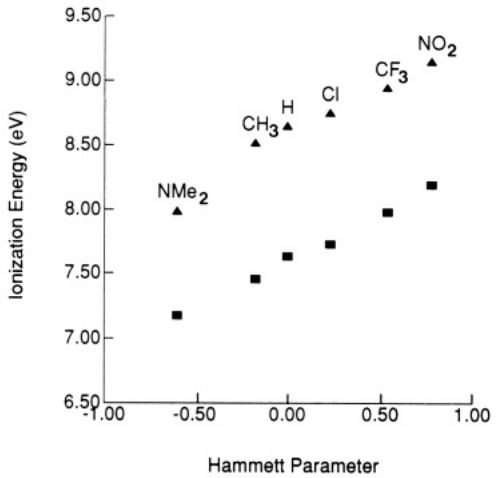

Figure 7. Plot of the M1 (■) and M2 (▲) ionization energies versus the Hammett σ_p parameters for the series of $(\eta^5\text{-}C_5H_4X)Rh(CO)_2$ compounds.

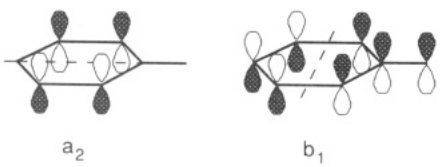

Figure 8. $1a_2$ and $2b_1$ orbitals of the π system in monosubstituted benzenes, showing p_π overlap with the X substituent.

activation ($\Delta\Delta G^\ddagger$) for the reaction is directly proportional to the $\Delta\Delta G$ for benzoic acid dissociation. Figure 7 shows that the M1 and M2 ionization potentials are reflecting a similar proportional change in energy. This might be expected, since ionization potentials are also measures of energy and are well-defined thermodynamic quantities that are part of chemical energy cycles.[18,19]

Ionization Energies and Orbital Overlap Interactions with the X Substituent. The electronic structure of monosubstituted cyclopentadienyl rings is directly analogous to that of monosubstituted benzenes, which have been studied extensively by photoelectron spectroscopy.[20,21] In benzene, the HOMO is the degenerate e_1 set of the π system. In monosubstituted benzenes (C_6H_5X), the e set splits into a_2 and b_1 levels (Figure 8). The functional group (X) affects the amount of shift and splitting of these levels, due to a combination of inductive and resonance effects. As the electron-donating ability (inductive effect) of X increases, both the b_1 and a_2 ionizations become more destabilized. If the substituent is capable of π donation to the ring, the b_1 ionization is further destabilized by p_π overlap interaction. Thus, the amount of splitting in the e set is a measure of the π orbital overlap interaction with the ring substituent.[20] In $(C_5H_5)Rh(CO)_2$, the e set of the cyclopentadienyl ring is already split because of interaction with the $Rh(CO)_2$ portion of the molecule. In the $(C_5H_4X)Rh(CO)_2$ compounds, the presence of functional groups on Cp causes both e_1 levels (R1 and R2) to shift, due to inductive effects. If the X group is capable of π donation, the R1 orbital is further destabilized. Thus, the

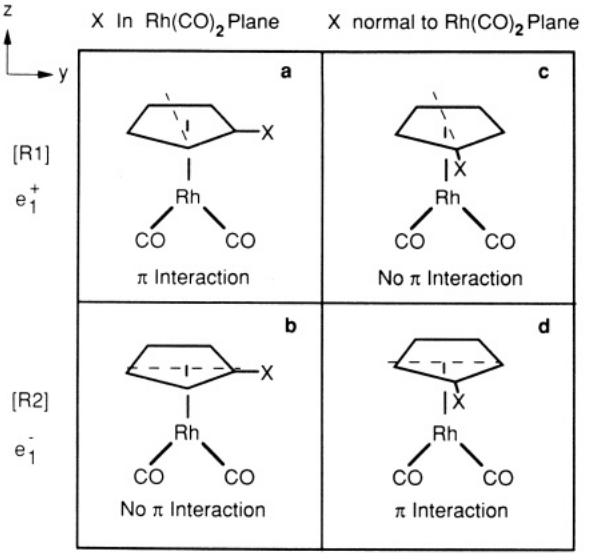

Figure 9. Interaction of the X substituent p_π orbital with the nodal planes of the R1 (Cp e_1^+) and R2 (Cp e_1^-) orbitals of $(\eta^5\text{-}C_5H_4X)Rh(CO)_2$ showing two possible orientations of the substituted Cp ring with the $Rh(CO)_2$ fragment.

degree of ring–substituent overlap can be seen in the increased splitting of R2 and R1 ionizations. The R2–R1 splitting (given in eV) is largest for the NMe_2 compound (1.732), followed by the Cl (1.144) and NO_2 (0.864) compounds, while the remaining compounds have values similar to that for the H compound (0.769).

The destabilization of the R1 orbital is the result of a filled–filled interaction between R1 and the lone-pair p_π orbital. This interaction is also reflected in the stabilization of the lone-pair ionization. In the spectrum of the NMe_2 compound, the ionization at 10.51 eV is attributed to the presence of the nitrogen p_π lone pair on the NMe_2 group. In comparison, the corresponding ionization of *N,N*-dimethylaniline is located at 9.83 eV.[22] Thus, there is a net stabilization of the nitrogen lone pair in $(\eta^5\text{-}C_5H_4NMe_2)Rh(CO)_2$, in spite of the effect of the formal negative charge on the Cp ring. It is interesting that NMe_2 apparently chooses to interact with R1 rather than R2. R2 is closer in energy to the nitrogen p_π lone pair, and the "choice" to interact with R1 minimizes the filled–filled repulsions by using the orbitals that have the larger energy separation.

In the spectrum of the $(\eta^5\text{-}C_5H_4Cl)Rh(CO)_2$ compound, the chlorine lone-pair ionizations also give direct evidence for overlap between the Cl p_π orbital and the Cp ring. As mentioned, the two ionizations that correspond to the lone-pair orbitals are located at 11.44 eV for the p_x orbital and 12.12 eV for p_π ($2b_1$). The significance of these positions is seen in a comparison with the photoelectron spectrum of chlorobenzene.[23] In chlorobenzene, a sharp band is located at 11.32 eV and corresponds to the chlorine p_x ($4b_2$) orbital. A second band, located at 11.70 eV, corresponds to the chlorine p_π ($2b_1$) orbital. The stabilization of the p_π orbital in $(\eta^5\text{-}C_5H_4Cl)Rh(CO)_2$ relative to chlorobenzene is the result of overlap with the Cp ring. The p_π orbital is also noticeably broadened in $(\eta^5\text{-}C_5H_4Cl)Rh(CO)_2$, indicating more bonding character. However, the extent of the overlap appears to be less for

(18) Lichtenberger, D. L.; Darsey, G. P.; Kellogg, G. E.; Sanner, R. D.; Young, V. G., Jr.; Clark, J. P. *J. Am. Chem. Soc.* **1989**, *111*, 5019.
(19) Lichtenberger, D. L.; Kellogg, G. E. *Gas Phase Inorganic Chemistry*; Plenum Press: New York, 1989; p 245.
(20) (a) Baker, A. D.; May, D. P.; Turner, D. W. *J. Chem. Soc. B* **1968**, 22. (b) Turner, D. W. *Philos. Trans. R. Soc. London, B* **1970**, 268, 7. (c) Turner, D. W.; Baker, C.; Baker, A. A.; Brundle, C. R. *Molecular Photoelectron Spectroscopy*; Wiley: New York, 1970.
(21) Debies, T. P.; Rabalais, J. W. *J. Electron Spectrosc. Relat. Phenom.* **1972**, *1*, 358.
(22) The value is from this work and represents a discrepancy from the literature value of 10.0 eV: Cowling, S. A.; Johnstone, R. A. W. *J. Electron. Spectrosc. Relat. Phenom.* **1973**, *2*, 161.
(23) Values of IP's are from this work and are in agreement with reported values: Potts, A. W.; Lyus, M. L.; Lee, E. P. F.; Fattahallah, G. H. *J. Chem Soc., Faraday Trans. 2* **1980**, *76*, 556.

the Cl compound than for the NMe_2 compound, which is expected for the longer bond distance and weaker π interaction of second-row atoms.

The orientation of the C_5H_4X ring with respect to the $Rh(CO)_2$ plane is suggested by the PE spectra. The inductive effect of the X group on the ionizations is relatively independent of the location of the X group on the Cp ring in relation to the $Rh(CO)_2$ plane. However, the π interaction of the X group with R1 depends on the location of the X group with respect to the nodal structure of the Cp e_1 levels. The e_1^+ or e_1^- nodes are defined first by their orientation to $Rh(CO)_2$ (Figure 2). Figure 9 shows the nodal structure of the monosubstituted Cp rings in terms of the interaction of the e_1^- and e_1^+ orbitals with an X group. Two limiting orientations available to the ring are (1) with the X group normal to the $Rh(CO)_2$ plane and (2) with the X group in the $Rh(CO)_2$ plane. In the first case, shown in Figure 9c,d, the X group has potential for a strong π interaction with the R2 level but is sitting on the node of the R1 level. In the second case, shown in Figure 9a,b, the situation is reversed and the X group has a π interaction with the R1 level. Because it is the R1 orbital that interacts with the lone-pair orbital, the NMe_2 substituent must lie near the CO–Rh–CO plane (the *yz* plane), as shown in Figure 9a.

Another observation from the NMe_2 spectrum is the extra destabilization of the M2 $d_{x^2-y^2}$ ionization. This is seen in the poorer correlation of M2 with the carbonyl stretching frequencies and in the smaller separation between M1 and M2 ionization bands. The destabilization of the M2 ($d_{x^2-y^2}$) ionization and the stabilization of the nitrogen lone-pair ionization are strong evidence of an additional filled–filled interaction between the nitrogen lone pair and the $d_{x^2-y^2}$ orbital. Such an interaction would be possible if NMe_2 either is in the $Rh(CO)_2$ plane or is normal to it. However, the shift of the Cp ring ionizations indicate that NMe_2 is in the $Rh(CO)_2$ plane. The extra destabilization of the M2 ($d_{x^2-y^2}$) band is not seen in the spectrum of the chlorine compound. Interaction of the chlorine lone pair with the $d_{x^2-y^2}$ orbital is less, perhaps because the C_5H_4Cl ring has an intermediate orientation (rotated about the *z* axis) or because of the longer C–Cl bond length as compared to the C–N bond length.

Ionization Energies and Reaction Rates. It is known that σ_p Hammett parameters do not correlate with rates of reactions in which resonance (π) interactions are present in the transition state.[17] This was observed in the $(C_5H_4X)Rh(CO)_2$ compounds, where the σ_p parameters did not correlate with the rates of associative substitution.[5] Several sets of parameters have been reported that attempt to separate the inductive (σ) and resonance (π) contributions to reaction rates.[24-26] Bromilow et al.[26] reported dual substituent parameters that represent measures of inductive (σ_I) and resonance (σ_R^0) effects. With use of these two parameters, a correlation with log $k(X)^*$ can be examined, where $k(X)^*$ is the rate constant for CO substitution in $(\eta^5\text{-}C_5H_4X)Rh(CO)_2$ compounds (the asterisk denotes that the values is relative to X = H). The equation, expressed in terms of σ_I and σ_R^0, has the form

$$\log k(X)^* = A[\sigma_I(X)] + B[\sigma_R^0(X)] \quad (2)$$

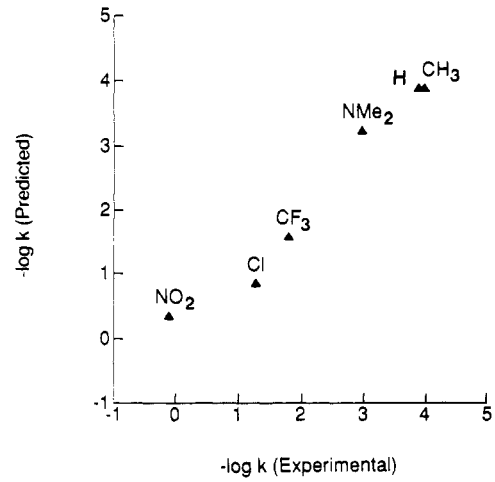

Figure 10. Dual-parameter correlation (using eq 2) of Hammett σ_I and σ_R^0 parameters with log k for CO substitution in $(\eta^5\text{-}C_5H_4X)Rh(CO)_2$ compounds (R = 0.9795).

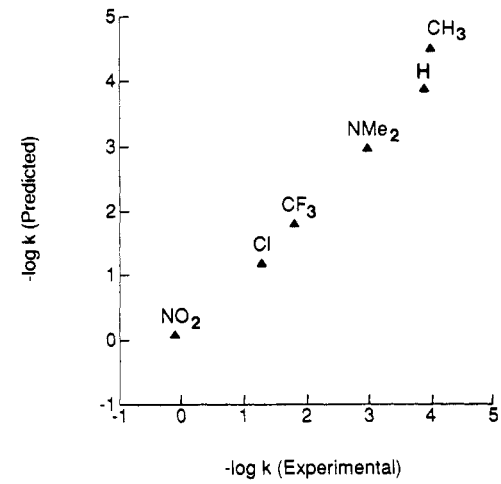

Figure 11. Correlation (using eq 3) of experimental rates of CO substitution with rates predicted from relative ionization potentials of the $(\eta^5\text{-}C_5H_4X)Rh(CO)_2$ compounds (R = 0.9914).

With these parameters and optimization of the coefficients A and B, the correlation with the rates of substitution is much better (correlation coefficient of 0.9795) than with σ_p alone.[5] A plot of the predicted versus the kinetically determined rates is shown in Figure 10. Parameters derived from other methods of separating the σ and π effects[24,26] give similar correlations.

An improved correlation with the rates of associative substitution is obtained when ionization potentials of the $(\eta^5\text{-}C_5H_4X)Rh(CO)_2$ compounds are used as measures of σ_I and σ_R^0 contributions. Equation 3 shows the "dual-parameter" correlation, with the values of the M2 ionization potentials as a measure of the inductive effect of X and the difference of R2 and R1 ionization potentials as a measure of the resonance effect. E_{M2}, E_{R1}, and E_{R2} are the ionization potentials of M2, R1, and R2 (relative to X = H), and C and D are optimized coefficients. The difference in R1 and R2 ionization potentials reflects the resonance (π) contribution to the rate of CO substitution. The M2 ionization energy was chosen as a measure of the σ (inductive) contribution of X for several reasons. The relative rate of substitution by an associative mechanism will be affected by the electron richness at the metal center, since a higher negative charge at the metal center will inhibit associative combination with the phosphine. The

$$\log k(X)^* = C[E_{M2}(X)]^* + D[E_{R2}(X) - E_{R1}(X)]^* \quad (3)$$

(24) (a) Taft, R. W.; Ehrenson, S.; Lewis, I. C.; Glick, R. E. *J. Am. Chem. Soc.* **1959**, *81*, 5352. (b) Ehrenson, S.; Brownlee, J.; Taft, R. W. *Prog. Phys. Org. Chem.* **1973**, *10*, 1.

(25) (a) Swain, C. G.; Unger, S. H.; Rosenquist, N. R.; Swain, M. S. *J. Am. Chem. Soc.* **1983**, *105*, 492. (b) Swain, M. S.; Lupton, E. C., Jr. *J. Am. Chem. Soc.* **1968**, *90*, 4328.

(26) Bromilow, J.; Brownlee, R. T. C.; Lopez, V. O.; Taft, R. W. *J. Org. Chem.* **1976**, *44*, 4766.

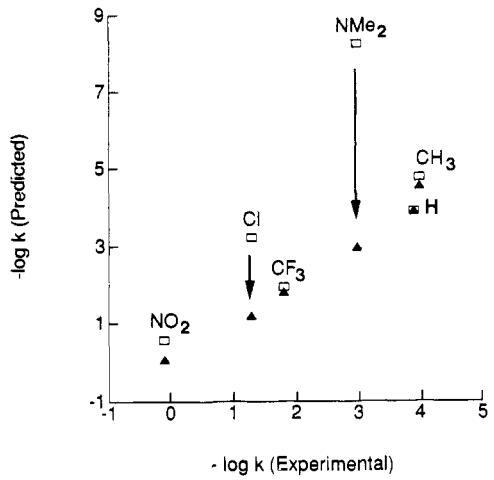

Figure 12. Illustration of the contribution of the π term to the prediction of the rates of CO substitution. The "□" symbols are the predicted rates with the σ term only, and the difference between the "□" and "▲" symbols represents the contribution of the π term to the predicted rate.

trends in the data show that both the M1 and M2 ionization energies are sensitive measures of the relative electron richness at the metal center. However, the M2 ionization is a better measure than the M1 ionization because M2 involves the $d_{x^2-y^2}$ orbital, which is presumably attacked by the incoming ligand and is involved in bonding in the piano-stool intermediate. The M2 ionization is also predominantly metal in character, while the M1 orbital is quite delocalized onto the Cp.

The resulting plot of predicted rate (from the relative ionization potentials) versus the kinetically observed rates (at 25 °C) is shown in Figure 11. The correlation coefficient (R) of 0.9914 is a marked improvement over the correlation for the σ_I and σ_R^0 Hammett parameters (Figure 10). The largest deviation is for the CH_3 compound. On the basis of what we have seen in other systems, the ionizations of the methyl compound show a smaller π contribution than is expected. This may be due to an intermediate geometry in the ground state, as discussed in the previous section.

The importance of the π contribution to the rates of NMe_2 and Cl compounds is notable when the "σ" part is ploted alone. Figure 12 shows the inductive contribution only, as defined by the first term $C[E_{M1}(X)]^*$, plotted versus the observed rates. This plot resembles the plot of the Hammett σ_p parameters versus log k,[5] where the points for X = Cl and NMe_2 are far off the line. When the π contributions are added, the points for NMe_2 and Cl fall onto the line. The plot shows little or no π contribution to the rate for CF_3 and CH_3. The plot also shows a π contribution for the NMe_2 compound which is 3 times that of the Cl compound. Since this p_π contribution is crucial to the correlation, a resonance interaction is implicated in the transition state. In the proposed mechanism, a p_π interaction would stabilize the slipped η^3-Cp ring intermediate and enhance the relative rate of associative substitution. It follows that certain X groups present on a Cp ring can stabilize an $(\eta^3\text{-}C_5H_4X)Rh(CO)_2(PPh_3)$ intermediate through p_π overlap and that the NMe_2 compound is very efficient at stabilizing an η^3-Cp intermediate.

The increased rates of associative substitution with π stabilization in these systems is also related to the ability of indenyl systems to enhance rates of associative substitution. The large rate enhancement (10^8 times) of indenyl over cyclopentadienyl is referred to as the indenyl ligand effect.[27b] The indenyl compound $(\eta^5\text{-}C_9H_7)Rh(CO)_2$ has carbonyl stretching frequencies nearly identical with those of $(\eta^5\text{-}C_5H_5)Rh(CO)_2$. Thus, the large rate enhancement cannot be caused by any inductive effects of indenyl. A large amount of p_π stabilization is present in an indenyl system, where an η^3-Cp ring is stabilized by a fused aromatic ring.[27] This additional p_π resonance interaction apparently stabilizes η^3 coordination in indenyl compounds, as there are more examples of structurally characterized η^3-indenyl rings[28] than of η^3-Cp rings.[29] This also accounts for the higher rates of substitution in the indenyl compounds.

Conclusions

This study demonstrates that photoelectron spectroscopy can be used to measure the relative inductive and resonance (π) bonding effects. In this system, the ionization energies of the metal and ligands are more direct measures for identifying inductive and resonance type bonding interactions than are the Hammett parameters. Both types of bonding interactions are important in describing the reactivity trends in the $(\eta^5\text{-}C_5H_4X)Rh(CO)_2$ compounds. Attaching electron-donating groups to the Cp ring results in more electron density at the metal center, which slows the rate of associative substitution. If however, a resonance π interaction between Cp and a functional group is present, the rate of substitution will increase. The ring–p_π overlap in the Cl and NMe_2 compounds appears to be a controlling factor in their enhanced rates of associative substitution. It is likely that a stabilized η^3-Cp intermediate is causing the rate enhancement in these systems and also in indenyl systems, where a "Cp" ring benefits from stabilization by a fused aromatic ring. This study also suggests that rates of other reactions which involved η^3-Cp intermediates[30] can be enhanced by attaching groups to the Cp ring that are capable of p_π orbital overlap.

Acknowledgment. D.L.L. acknowledges support by the U.S. Department of Energy (Division of Chemical Sciences, Office of Basic Energy Sciences, Office of Energy Research; Contract No. DE-FG02-86ER13501) for the study of the electronic structure of organometallic molecules, the National Science Foundation (Grant No. CHE-8519560) for the study of ionization-reactivity relationships, and the Materials Characterization Program, Department of Chemistry, University of Arizona, for assistance with maintenance of the instrumentation. F.B. acknowledges the National Science Foundation (Grant No. CHE-8514366). We are grateful to the Johnson Matthey Corp. for their generous loan of the rhodium used in this study.

(27) (a) Hart-Davis, A. J.; White, C.; Mawby, R. J. *Inorg. Chim. Acta* **1970**, *4*, 441. (b) Ji, L. N.; Rerek, M. E.; Basolo, F. *Organometallics* **1984**, *3*, 740. (c) Habib, A.; Tanke, R. S.; Holt, E. M.; Crabtree, R. H. *Organometallics* **1989**, *8*, 1225.

(28) (a) $(\eta^3$-fluorenyl$)(\eta^5$-fluorenyl$)ZrCl_2$; Kowala, C.; Wunderlich, J. A. *Acta Crystallogr., Sect. B* **1976**, *B32*, 820. (b) $(\eta^3$-ind$)(\eta^5$-ind$)W(CO)_2$; Nesmeyanov, A. N.; Ustynyuk, L. G.; Makorova, L. G.; Andrianov, V. G.; Struchkov, Yu. T.; Andre, S. *J. Organomet. Chem.* **1978**, *159*, 189. (c) $(\eta^3$-ind$)Ir(PMe_2Ph)_3$; Merola, J. S.; Kacmarick, R. T.; Van Eagen, D. *J. Am. Chem. Soc.* **1986**, *108*, 329. (d) $(\eta^3$-ind$)(\eta^5$-ind$)V(CO)_2$; Kowaleski, R. M.; Rheingold, A. L.; Trogler, W. C.; Basolo, F. *J. Am. Chem. Soc.* **1986**, *108*, 2461.

(29) (a) $(\eta^5\text{-}C_5H_5)(\eta^3\text{-}C_5H_5)W(CO)_2$; Huttner, G.; Brintzinger, H. H.; Bell, L. G.; Friedrich, P.; Bejenke, V.; Neugebauet, D. *J. Organomet. Chem.* **1978**, *145*, 329. (b) $[(\eta^5\text{-}C_5Me_5)(\eta^3\text{-}C_5Me_5)Al(Cl)(R)]_2$; Schonberg, P. P.; Paine, R. T.; Campana, C. F.; Duesler, E. N. *Organometallics* **1982**, *1*, 799.

(30) (a) Cramer, R.; Siewell, L. P. *J. Organomet. Chem.* **1975**, *92*, 245. (b) Yang, G. K.; Bergman, R. G. *Organometallics* **1985**, *4*, 129. (c) Rest, A. J.; Whitwell, I.; Graham, W. A. G.; Hoyano, J. K.; McMaster, A. D. *J. Chem. Soc., Chem. Commun.* **1984**, 624.